Epitaxial growth and magnetic characterization of ferromagnetic Co4N thin films on SrTiO3(001) substrates by molecular beam epitaxy

著者別名	都甲 薫, 末益 崇
journal or publication title	Journal of crystal growth
volume	336
number	1
page range	40-43
year	2011-12
権利	(C) 2011 Elsevier B.V. NOTICE: this is the author ’ s version of a work that was accepted for publication in Journal of crystal growth. Changes resulting from the publishing process, such as peer review, editing, corrections, structural formatting, and other quality control mechanisms may not be reflected in this document. Changes may have been made to this work since it was submitted for publication. A definitive version was subsequently published in Journal of crystal growth, 336, 1, 2011 DOI:10.1016/j.jcrysgro.2011.09.038
URL	http://hdl.handle.net/2241/114807

doi: 10.1016/j.jcrysgro.2011.09.038

Epitaxial growth and magnetic characterization of ferromagnetic Co_4N thin films on $SrTiO_3$(001) substrates by molecular beam epitaxy

Keita Ito[a], Kazunori Harada[a], Kaoru Toko[a], Hiro Akinaga[b], Takashi Suemasu[a]

[a]*Institute of Applied Physics, University of Tsukuba, 1-1-1 Tennohdai, Tsukuba, Ibaraki 305-8573, Japan*

[b]*National Institute of Advanced Industrial Science and Technology (AIST), ICAN, 16-1 Onogawa, Tsukuba, Ibaraki 305-8569, Japan*

Keywords: Molecular beam epitaxy, Spintronics, Ferromagnetic material, Co_4N, $SrTiO_3$

We have attempted to grow single-crystalline Co_4N thin films on $SrTiO_3$ (STO) (001) substrates by molecular beam epitaxy by the simultaneous supply of 3N-Co and radio-frequency NH_3 plasma. Reflection high-energy electron diffraction and θ-2θ x-ray diffraction patterns confirmed that the epitaxial growth of Co_4N films was successfully

achieved. X-ray ϕ-scan measurements using Co_4N(301) and STO(301) diffractions revealed that the epitaxial relationship between Co_4N and STO was a cube-on-cube type. Magnetization versus magnetic field curves measured at room temperature for Co_4N epitaxial layers covered with a Au capping layer using a vibrating sample magnetometer showed that Co_4N[110] is the axis of easy magnetization.

1. Introduction

Spintronics aims to achieve new functional devices utilizing the spin degree of freedom and has attracted significant attention in recent years. High efficiency spin injection from ferromagnetic materials to non-magnetic materials is of significant importance to realize new spintronics devices, such as spin transistors. Therefore, much research has been conducted to identify ferromagnetic materials with large spin polarization (*P*) from both a theoretical and experimental aspect. Iron nitrides, which consist of abundantly available nontoxic atoms, are regarded as promising materials for application in magnetic recording media. Among them, Fe_4N has been extensively studied over the past few years. A large *P* value of electrical conductivity (σ) due to up and down spins at the Fermi level, given by $(\sigma_{\uparrow} - \sigma_{\downarrow}) / (\sigma_{\uparrow} + \sigma_{\downarrow})$, was theoretically predicted to be –1.0 [1]. We have confirmed from point contact Andreev reflection measurements that Fe_4N layers grown by molecular beam epitaxy (MBE) on MgO(001) substrates have a distinctly larger *P* than that of α-Fe [2]. We also evaluated the spin and orbital magnetic moments of Fe_4N epitaxial thin films from X-ray magnetic circular dichroism measurements [3]. In contrast, there have been no reports on the formation of Co_4N single-crystalline epitaxial films, nor their magnetic properties. Co_4N has a cubic perovskite lattice structure, where one N atom is located at the body-center of fcc-Co, and the lattice constant is reported to be 0.3738 nm [4]. There have been only a limited number of reports on the growth of cobalt nitride

(Co-N) films by sputtering [5-7]. Very recently, Imai *et al*. calculated that the *P* value of the density of states (*D*) for up and down spins at the Fermi level, described by ($D_\uparrow$ - $D_\downarrow$) / ($D_\uparrow$ + $D_\downarrow$), reaches approximately –0.88, and this value is larger than that of Fe_4N (–0.67) [8]. Therefore, Co_4N is also considered as a promising material for application to spintronics devices. The formation and characterization of high-quality Co_4N epitaxial films is necessary to confirm the theoretically predicted features of Co_4N.

In this study, we attempted to grow Co_4N epitaxial films on $SrTiO_3$ (STO) (001) substrates by MBE. Furthermore, magnetization versus magnetic field (*M*-*H*) curves were measured using a vibrating sample (VSM) and superconducting quantum interface device (SQUID) magnetometers, and the saturation magnetization (M_s), coercive field (H_c) and magnetic anisotropy of Co_4N thin films were evaluated. There have been no reports so far on the epitaxial growth of Co_4N thin films by MBE, so that the magnetic anisotropy of Co_4N has yet to be clarified.

2. Experimental procedures

An ion-pumped MBE system equipped with a high-temperature Knudsen cell for 3N–Co and a radio-frequency (RF) 5N–NH_3 plasma for N was used. Co_4N layers were grown by MBE with simultaneous supply of solid Co and NH_3 plasma on the STO(001) substrate. We have recently utilized the same growth method and succeeded in the epitaxial growth of

Fe_4N thin films [9]. Prior to the growth of Co_4N, the STO(001) substrates were immersed into a buffered HF (HF = 5 wt%, NH_4F = 35 wt%) solution to obtain an atomically flat surface [10]. The growth conditions for sample preparation are summarized in Table 1. Co_4N thin films (samples A–C) were grown at 450, 400 and 350 °C, respectively. During the growth of Co_4N, the deposition rate of Co was kept constant at approximately 0.5 nm/min. The flow rate of NH_3 was fixed at 1.0 sccm, and the input power to the RF plasma was 150 W. The pressure inside the chamber was approximately 1×10^{-4} Torr during film growth. For the preparation of sample D, the Co_4N layer was capped with a 7 nm thick Au layer by MBE to prevent oxidation of the surface.

The crystalline qualities of the samples were characterized by reflection high-energy electron diffraction (RHEED) and θ-2θ X-ray diffraction (XRD) measurements. The surface roughnesses of Co_4N layers were observed using atomic force microscopy (AFM). The epitaxial face relationship between Co_4N and STO was determined by ϕ-scan XRD using Co_4N(301) and STO(301) diffractions. Cu K_α X-rays were used for XRD measurements. *M*-*H* curve measurements were performed on sample D using the VSM and SQUID at room temperature. An external magnetic field (*H*) was applied parallel to sample surfaces.

3. Results and discussion

Figures 1(a) and 1(b) show RHEED patterns of sample B for the electron beam incident along the [100] and [110] directions of STO, respectively. Similar RHEED patterns were also observed for Co_4N layers in other samples. Predicted transmission electron diffraction patterns for Co_4N are also shown for comparison. Spotty RHEED patterns indicate that the surface of the grown layer is rough, probably due to the large lattice mismatch of 4.3% between Co_4N and STO. The experimentally obtained RHEED patterns resemble the predicted diffraction patterns. X-ray ϕ-scan measurements indicated that the grown layers were not fcc-Co, but Co_4N, which is discussed in detail later. At the present stage, it can at least be stated from the RHEED patterns that the grown layers have a single crystalline nature.

Figure 2 shows the θ-2θ XRD patterns of samples A–C. No diffraction peaks corresponding to fcc-Co or Co-N, other than *c*-axis oriented Co_4N, were observed. There was no significant difference in crystalline qualities such as RHEED and XRD among samples A–C. The *c*-axis lattice constant of Co_4N in sample B was determined to be 0.3524 nm. To reduce the measurement error, lattice constants deduced from Co_4N(002) and Co_4N(004) peak positions were first plotted against $\cot\theta$ after canceling zero offset error by adjusting the measured peak position of STO with the theoretical peak position. The peak positions were determined by Gaussian fitting. The *c*-axis lattice constant of Co_4N was then extrapolated from the intersection of the straight line passing through the above two points at $\cot\theta = 0$. This value of 0.3524 nm is slightly smaller than the reported value of 0.3738 nm, which indicates that the grown Co_4N film is under tensile strain along the in-plane direction. This is due to a larger lattice constant of STO than that of Co_4N. The lattice constant of fcc-Co (0.3544 nm) [6] is very close to that of Co_4N films on glass slides (0.3586 nm) [5]; thus, it is difficult to state that the grown film is Co_4N solely from the peak positions in the XRD pattern shown in Fig. 2. However, we can exclude the possibility of fcc-Co by considering the ϕ-scan XRD measurement shown in Fig. 3(a).

ϕ-scan XRD measurement was performed to investigate the epitaxial face relationship between Co_4N and STO. Figure 3(a) shows the ϕ-scan XRD pattern for $Co_4N(301)$ and STO(301) diffraction peaks measured on sample B. The peaks of both $Co_4N(301)$ and STO(301) were observed at the same ϕ positions with 90° intervals; therefore, the epitaxial face relationship between these two materials is a cube-on-cube type, as shown in Fig. 3(b). According to the X-ray extinction law, the diffraction peak of fcc-Co(301) is forbidden; however, that of $Co_4N(301)$ is allowed. Therefore, we can state that the grown layers are not fcc-Co, but Co_4N. On the basis of these experimental results, we have concluded that *c*-axis oriented Co_4N epitaxial films were successfully grown, for the first time, on STO(001) substrates.

Figure 4 shows the growth temperature dependence of root-mean-square (RMS) values of surface roughness in samples A–C. RMS values of the surface roughness slightly increased with increasing growth temperature of Co_4N layers. But there was no significant difference in RMS roughness value between samples B and C. Thus, we chose the growth temperature of 400 °C and prepared sample D for magnetic measurements.

Figure 5(a) and 5(b) show *M*-*H* curves and incident *H* angle dependence of the ratio of remanent magnetizations (M_r) to M_s measured for sample D, respectively. Vertical axis in Fig. 5(a) is the magnetization (*M*) normalized by the M_s of sample D. H_c is approximately 25 Oe, which indicates that Co_4N is a soft magnetic material. The crystalline magnetic anisotropy was observed as shown in Fig. 5(b). M_r differed depending on the directions of applied external *H*. M_r/M_s was equivalent to 1.0 when the external *H* was parallel to Co_4N[110]. In contrast, M_r/M_s decreases to approximately 0.75 when the external *H* was applied parallel to Co_4N[100] and [010]. These results indicate that the in-plane [110] direction is an easy magnetization axis of *c*-axis-oriented Co_4N film, as it is for fcc-Co [11]. The M_s value was calculated to be approximately 1300 emu/cc at 300 K using a SQUID magnetometer, corresponding to approximately 1.6 μ_B per Co atom. This value is close to that theoretically predicted [8].

4. Conclusions

Single-crystalline *c*-axis-oriented epitaxial Co_4N thin films were successfully grown on STO(001) substrates by MBE with the simultaneous supply of solid Co and RF-NH_3. Co_4N thin films on STO are under slight tensile strain, where the in-plane lattice is extended. A cube-on-cube epitaxial relationship was confirmed between Co_4N and STO(001) from ϕ-scan XRD measurements using Co_4N(301) and STO(301) diffraction peaks. Co_4N[110] was found to be an easy axis of magnetization from *M*-*H* measurements obtained using a VSM.

Acknowledgements

This work was supported in part by a Grant-in-Aid for Scientific Research on the Priority Area of "Creation and Control of Spin Current" (19048030) from the Ministry of Education, Culture, Sports, Science and Technology of Japan (MEXT) and by the NanoProcessing Partnership Platform (NPPP) at the National Institute for Advanced Industrial Science and Technology (AIST), Tsukuba. ϕ-scan XRD measurements were performed with the help of the Rigaku Corporation. *M*-*H* curve measurements were performed with the cooperation of Dr. H. Yanagihara, Dr. T. Koyano and Prof. E. Kita of the University of Tsukuba. The authors also thank Dr. N. Ota and Prof. K. Asakawa of the Tsukuba Nano-Tech Human Resource Development Program at the University of Tsukuba for useful discussions.

References

[1] S. Kokado, N. Fujima, K. Harigaya, H. Shimizu, A. Sakuma, Phys. Rev. B 73 (2006) 172410.

[2] A. Narahara, K. Ito, T. Suemasu, Y. K. Takahashi, A. Rajanikanth, K. Hono, Appl. Phys. Lett. 94 (2009) 202502.

[3] K. Ito, G. H. Lee, K. Harada, M. Suzuno, T. Suemasu, Y. Takeda, Y. Saitoh, M. Ye, A. Kimura, H. Akinaga, Appl. Phys. Lett. 98 (2011) 102507.

[4] N. Terao, Mem. Sci. Rev. Met. 57 (1960) 96.

[5] K. Oda, T. Yoshio, K. Oda, J. Mater. Sci. 22 (1987) 2729.

[6] J. S Fang, L. C. Yang, C. S. Hsu, G. S. Chen, Y. W. Lin, G. S. Chen, J. Vac. Sci. Technol. A 22 (2004) 698.

[7] H. Jia, X. Wang, W. Zheng, Y. Chen, S. Feng, Mater. Sci. Eng. B 150 (2008) 121.

[8] Y. Imai, Y. Takahashi, T. Kumagai, J. Magn. Magn. Mater. 322 (2010) 2665.

[9] K. Ito, G. H. Lee, H. Akinaga, T. Suemasu, J. Cryst. Growth. 322 (2011) 63.

[10] M. Kawasaki, K. Takahashi, T. Maeda, R. Tsuchiya, M. Shinohara, O. Ishiyama, T. Yonezawa, M. Yoshimoto, H. Koinuma, Science 266 (1994) 1540.

[11] B. Heinrich, J. F. Cochran, M. Kowalewski, J. Kirschner, Z. Celinski, A. S. Arrott, K. Myrtle, Phys. Rev. B 44 (1991) 9348.

Fig. 1. RHEED patterns for grown layers of sample B measured from the (a) [100] and (b) [110] azimuths of STO. Lower patterns are predicted transmission electron diffraction patterns.

Fig. 2. θ-2θ XRD patterns for samples A–C.

Fig. 3. (a)ϕ-scan XRD patterns for Co_4N(301) and STO(301) in sample B. (b) Epitaxial relationship between Co_4N and STO.

Fig. 4. The growth temperature dependence of RMS values of surface roughness in samples A–C.

Fig. 5. (a)*M*-*H* curves and (b)incident *H* angle dependence of M_r/M_s for samples D measured at 300 K. External *H* were applied to the [010] and [110] azimuths of Co_4N parallel to the sample surface.

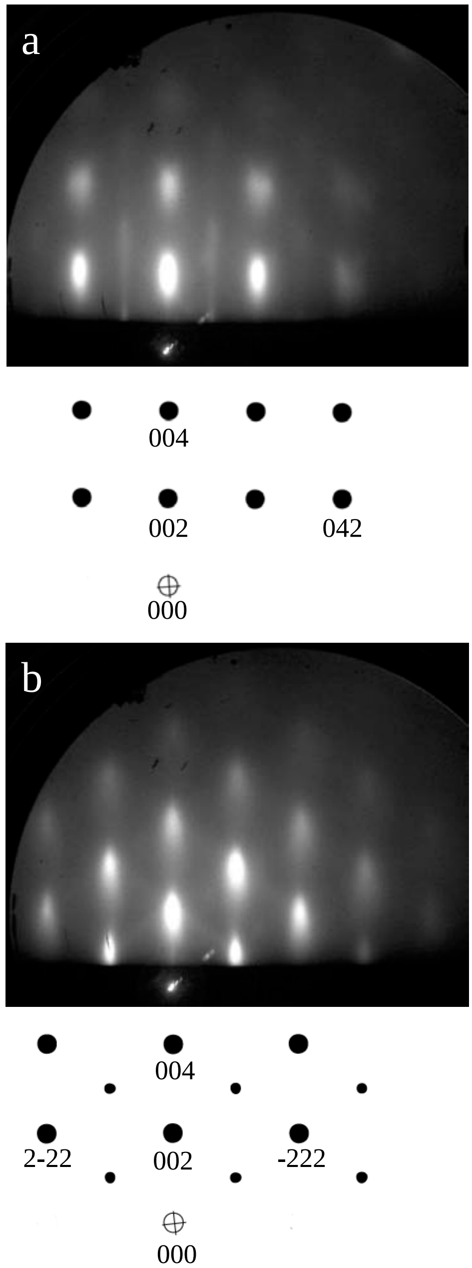

Fig. 1

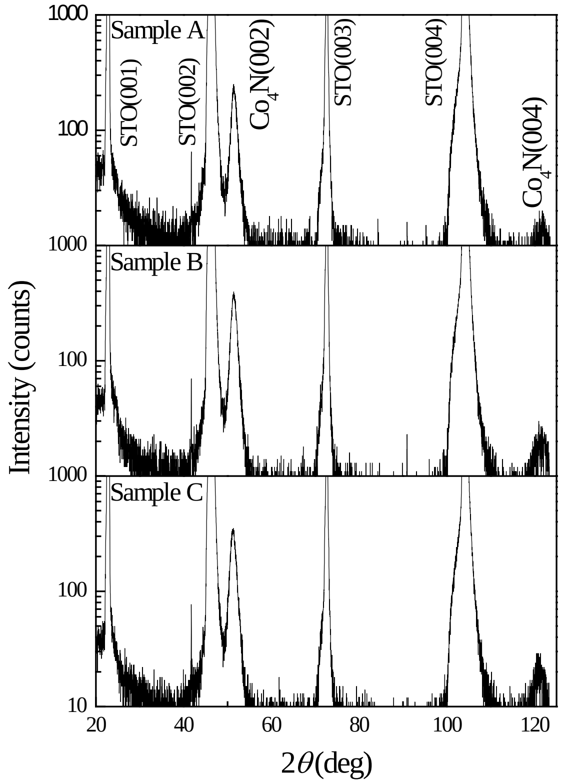
Sample A
STO(001)
STO(002)
Co$_4$N(002)
STO(003)
STO(004)
Co$_4$N(004)
Sample B
Sample C
Intensity (counts)
1000
100
10
20
40
60
80
100
120
2θ(deg)

Fig. 2

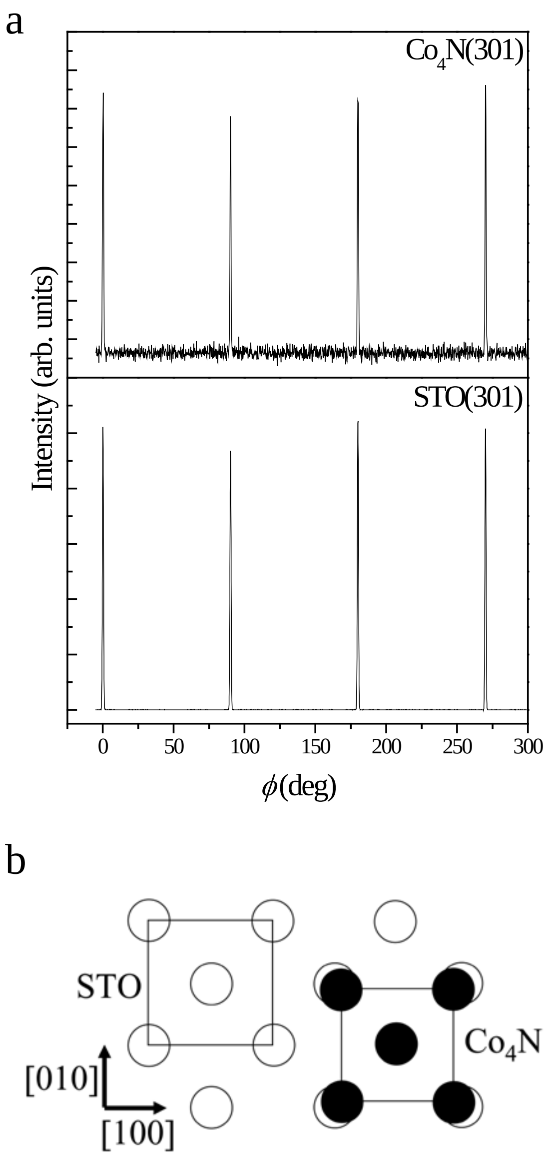
a
Co4N(301)
STO(301)
Intensity (arb. units)
0
50
100
150
200
250
300
φ(deg)
b
STO
Co4N
[010]
[100]

Fig. 3

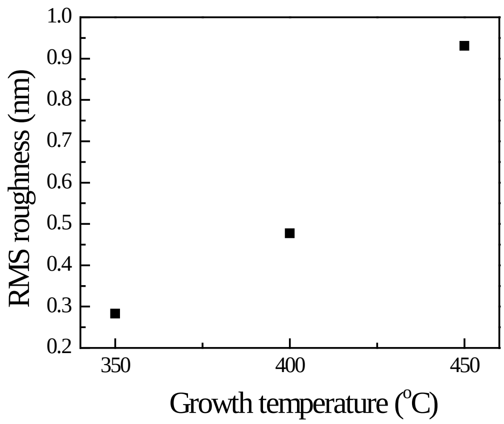

1.0
0.9
0.8
0.7
0.6
0.5
0.4
0.3
0.2
RMS roughness (nm)
350
400
450
Growth temperature (oC)

Fig.4

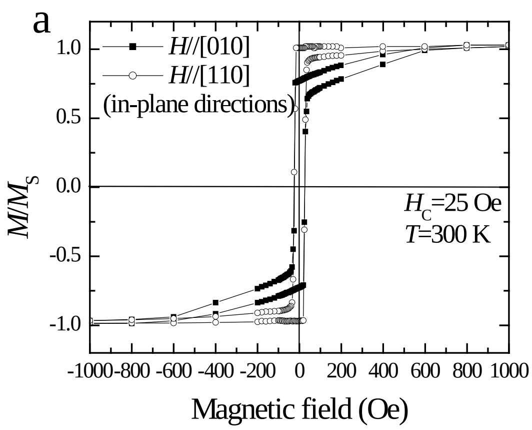
a
H//[010]
H//[110]
(in-plane directions)
H_C=25 Oe
T=300 K
M/M_S
Magnetic field (Oe)
1.0
0.5
0.0
-0.5
-1.0
-1000
-800
-600
-400
-200
0
200
400
600
800
1000

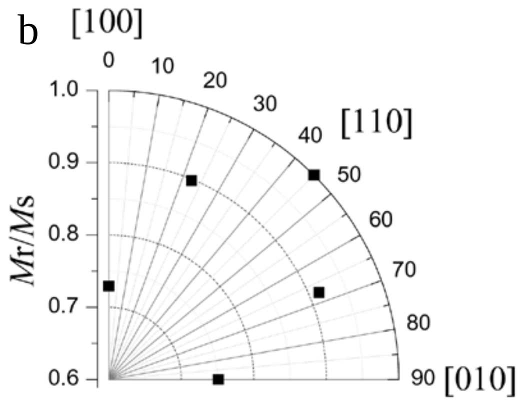
b
[100]
[110]
[010]
Mr/Ms
0
10
20
30
40
50
60
70
80
90
1.0
0.9
0.8
0.7
0.6

Fig. 5

Table 1 Growth conditions used for sample preparation. Samples A–D were grown on STO substrates. The Co_4N layer was covered with a 7-nm-thick Au capping layer in sample D.

Sample	Substrate	Growth temperature (°C)	Co_4N layer (nm)	Au layer (nm)
A	STO(001)	450	13	-
B	STO(001)	400	14	-
C	STO(001)	350	13	-
D	STO(001)	400	9	7